Chemical Science

EDGE ARTICLE

View Article Online
View Journal | View Issue

Cite this: *Chem. Sci.*, 2014, **5**, 1046

Tuning "thiol-ene" reactions toward controlled symmetry breaking in polyhedral oligomeric silsesquioxanes†

Yiwen Li,‡[a] Kai Guo,‡[a] Hao Su,[a] Xiaopeng Li,[b] Xueyan Feng,[a] Zhao Wang,[a] Wei Zhang,[a] Sunsheng Zhu,[a] Chrys Wesdemiotis,*[ab] Stephen Z. D. Cheng*[a] and Wen-Bin Zhang*[ac]

Received 29th September 2013
Accepted 18th November 2013

DOI: 10.1039/c3sc52718b

www.rsc.org/chemicalscience

The convenient synthesis of nano-building blocks with strategically placed functional groups constitutes a fundamental challenge in nano-science. Here, we describe the facile preparation of a library of mono- and di-functional (containing three isomers) polyhedral oligomeric silsesquioxane (POSS) building blocks with different symmetries (C_{3v}, C_{2v}, and D_{3d}) using thiol-ene chemistry. The method is straightforward and general, possessing many advantages including minimum set-up, simple work-up, and a short reaction time (about 0.5 h). It facilitates the precise introduction of a large variety of functional groups to desired sites of the POSS cage. The yields of the monoadducts increase significantly using stoichiometric amounts of bulky ligands. Regio-selective di-functionalization of the POSS cage was also attempted using bulky thiol ligands, such as a thiol-functionalized POSS. Electrospray ionization (ESI) mass spectrometry coupled with travelling wave ion mobility (TWIM) separation revealed that the majority of diadducts are *para*-compounds (~59%), although *meta*-compounds (~20%) and *ortho*-compounds (~21%) are also present. Therefore, the thiol-ene reaction provides a robust approach for the convenient synthesis of mono-functional POSS derivatives and, potentially, of regio-selective multi-functionalized POSS derivatives as versatile nano-building blocks.

Introduction

The past decades have witnessed the creative use of "bottom-up" strategies for the design and synthesis of a large variety of nano-structured functional materials.[1,2] Many of them, such as small-molecule surfactants,[3,4] block copolymers[5,6] and Janus particles[7,8] possess amphiphilic character, which acts as the driving force for their self-assembly. A relatively recent addition is a class of hybrid materials named "shape amphiphiles" that possess amphiphilic features in shape – they consist of molecular segments that have incommensurate shape and competing interactions.[9–13] Molecular nano-particles (MNPs), such as fullerene,[14,15] polyoxometalate (POM)[16,17] and T_8 polyhedral oligomeric silsesquioxane (POSS),[18–22] have been widely used as versatile building blocks for the construction of various shape amphiphiles with controlled surface chemistry and macromolecular architectures.[23–29] The most important character of the amphiphilic molecules is symmetry breaking. In shape amphiphiles, symmetry breaking can be simply achieved by coupling MNP building block precursors in different geometrical ways. It is thus critical to have a library of readily available MNP building blocks with an exact number of surface functional groups at precise locations, in order to enable the synthesis of diverse shape amphiphiles *via* both "grafting-from"[12,27] and "grafting-onto" strategies.[25,26,28,29]

Site-selective functionalization and regio-selective multi-functionalization of MNPs are non-trivial. Fullerene chemistry has been thoroughly studied and documented in this respect.[30] The principles underlying its functionalization strategies shall be equally applicable to other MNPs. For the preparation of monoadducts, control of the reaction stoichiometry is a straightforward solution if the purification of monoadducts is possible by either chromatographic or non-chromatographic methods. For regio-selective multi-addition on C_{60}, strategies like template-mediated multi-addition, topochemically-controlled solid-state reaction, and tether-directed remote functionalization have been well established.[30] The spherical shape and I_h symmetry of C_{60} are broken to generate a variety of multifunctional fullerene building blocks.[31,32] In contrast,

[a]*Department of Polymer Science, College of Polymer Science and Polymer Engineering, The University of Akron, Akron, Ohio 44325-3909, USA. E-mail: wenbin@pku.edu.cn; wesdemiotis@uakron.edu; scheng@uakron.edu; Fax: +86 10 6275 1708; +1 330 972 8626; +1 330 972 6085; Tel: +86 10 6275 2394; +1 330 972 6931; +1 330 972 7699*

[b]*Department of Chemistry, The University of Akron, Akron, Ohio 44325-3601, USA*

[c]*Department of Polymer Science and Engineering, College of Chemistry and Molecular Engineering, Center for Soft Matter Science and Engineering, Peking University, Beijing 100871, China*

† Electronic supplementary information (ESI) available: Details of characterization data including the synthesis and characterization of the compounds. See DOI: 10.1039/c3sc52718b

‡ These authors contributed equally to this work.

similar strategies have not been fully demonstrated in the preparation of POSS-based nanobuilding blocks, especially for the regio-selective modification of POSS with reactive side groups (such as vinyl side groups) instead of inert side groups (such as alkyls).[20,33,34]

Mono-functionalization of T_8 POSS breaks the O_h symmetry of POSS to a C_{3v} symmetry. So far, there are mainly three ways to do so: (1) co-hydrolysis of tri-functional organo- or hydrosilanes;[35,36] (2) corner-capping reactions;[37,38] and (3) the selective side group modification of an intact POSS cage.[39,40] However, these methods are largely limited to those POSS compounds with seven inert periphery groups, imposing significant hurdles for further functionalization to form diverse building blocks. Feher and co-workers have demonstrated the mono-hydroxylation of octavinylPOSS to prepare a versatile intermediate, VPOSS-OH.[41] The vinyl and hydroxyl groups possess orthogonal reactivities, allowing sequential functionalization of VPOSS-OH into a large variety of shape amphiphiles.[23] Yet, the synthesis cannot be easily adapted for the preparation of mono-functional POSS with other reactive groups. Recently, Chiara *et al.* used stoichiometry-controlled copper-catalyzed azide–alkyne cycloaddition (CuAAC) of octakis(3-azidopropyl)octasilsesquioxane as an effective and powerful way to prepare mono-functional POSSs.[42,43] The use of this classic "click" reaction greatly improved the functional group tolerance during functionalization and the remaining azido groups could be easily derivatized into other functional groups.[42] To further expand the scope of POSS-based building blocks, we aim to apply other "click" chemistry reactions and develop a general and convenient method for the preparation of POSS derivatives with relatively simple linker groups (as compared to the triazole ring).

Thiol-ene chemistry has also been recognised as a typical "click" reaction. The anti-Markovnikov addition occurs rapidly and efficiently under mild conditions even in the presence of oxygen and water. Simultaneously, multiple functionalization of octavinylPOSS has been shown to be extremely effective in tuning the surface functionalities on POSS cages from hydrophilic groups[8,12,24,25,27] to fluorophilic functionalities,[8,44] and even to bioactive moieties.[12,45] The thiol-ene addition of 1-thioglycerol to an equimolar amount of octavinylPOSS leads predominantly to a monoadduct that can be purified by flash chromatography.[27] In this manuscript, we report a systematic study on the use of thiol-ene chemistry[46–50] for the controlled functionalization of octavinylPOSS cages. The method is broad in scope and convenient in practice. Both the mono-functionalization and the multi-functionalization have been explored in detail.

Results and discussion

We first examined the scope of the method by using a library of functional thiols. Scheme 1 shows the synthesis of mono-functional heptavinylPOSSs (VPOSS-S-R) **14–26** in one step from these thiols. The thiols were designed to diversify the functional properties of the final shape amphiphiles. Thiols **1** to **7** can be employed to introduce common reactive functionalities on the POSS cage in a single step, including hydroxyl, carboxylic acid, amine, bromo, and azido groups. Both the length of the linker group and the number of functional groups at one single corner of POSS can be varied, as demonstrated by using different hydroxyl-functionalized thiols [2-mercaptoethanol (**1**), 6-mercapto-1-hexanol (**2**), and 1-thioglycerol (**3**)]. Beyond the common reactive groups, it is worth mentioning that the functional thiol **6** (Br-SH) contains a 2-bromoisobutyryl moiety that can be used to initiate atom transfer radical polymerization (ATRP) for the efficient "grafting" of a polymer chain from the vinyl POSS surface,[27] while thiol **7** (N_3-SH) could be used to introduce a "clickable" group on POSS for the subsequent "grafting" of another macromolecular building block onto the vinyl POSS cage through a Huisgen [3 + 2] cycloaddition.[51] Thiol **8** (AD-SH) contains an adamantane motif that can form a complex with a cyclodextrin host *via* non-covalent interactions,[52,53] which could enable the preparation of supramolecular shape amphiphiles.[54] The ferrocene moiety in thiol **9** (Fe-SH) imparts redox properties to the building block and may facilitate the design and synthesis of smart shape amphiphiles.[55,56] Other bioactive molecules, such as sugars, can also be introduced by using thiols like Sugar-SH **10**. Finally, a series of relatively bulky thiol ligands that bear a second nano-building block, such as a small dendron (Dendron-SH **11**)[57] or isobutyl functionalized POSS with different linkers (BPOSS-SH **12** and BPOSS-NHCO-SH **13**), have also been designed. Among the thiols in Scheme 1, the ligands **1–5**, **10** and **12** are commercially available while ligands **6–9**, **11** and **13** were synthesized in our laboratory (see ESI†). Thiols **7–9**, **11** and **13** are new compounds and were conveniently prepared from carboxylic acid-functionalized precursors.

To perform the reaction, equimolar amounts of a functional thiol and octavinylPOSS were simply mixed in a common solvent (such as THF, DMF, or $CHCl_3$) in the presence of 2 mol% of 2,2-dimethoxy-2-phenylacetophenone (DMPA, photoinitiator) at a octavinylPOSS concentration of 10 mg mL^{-1} and the mixture was irradiated under a UV 365 nm lamp at room temperature for about 30 min. After solvent removal, the monoadduct was purified by flash chromatography in 20–41% yield. Notably, ~30–50% of octavinylPOSS could often be recovered and thus, the effective yields of the monoadducts based on conversions are much higher. The yields could be further improved if experimental conditions were further optimized by varying the octavinylPOSS concentration and/or the stoichiometry.[42] However, for the sake of convenience, we consistently used a stoichiometry of 1 : 1 and a concentration of 10 mg mL^{-1} of octavinylPOSS.[42] The purification of VPOSS-S-R takes advantage of the difference in polarity among the starting materials, the monoadducts, and the multi-adducts. Generally, VPOSS-S-R samples were easily separated from octavinylPOSS, the photoinitiator and the multi-adducts in good yields, providing a set of mono-functional POSS units for further modification.

The products, VPOSS-S-R **14–26**, were named and numbered in accordance to the thiol precursor, respectively (see Table 1 and ESI†). They were thoroughly characterized by NMR spectroscopy and mass spectrometry to confirm their molecular

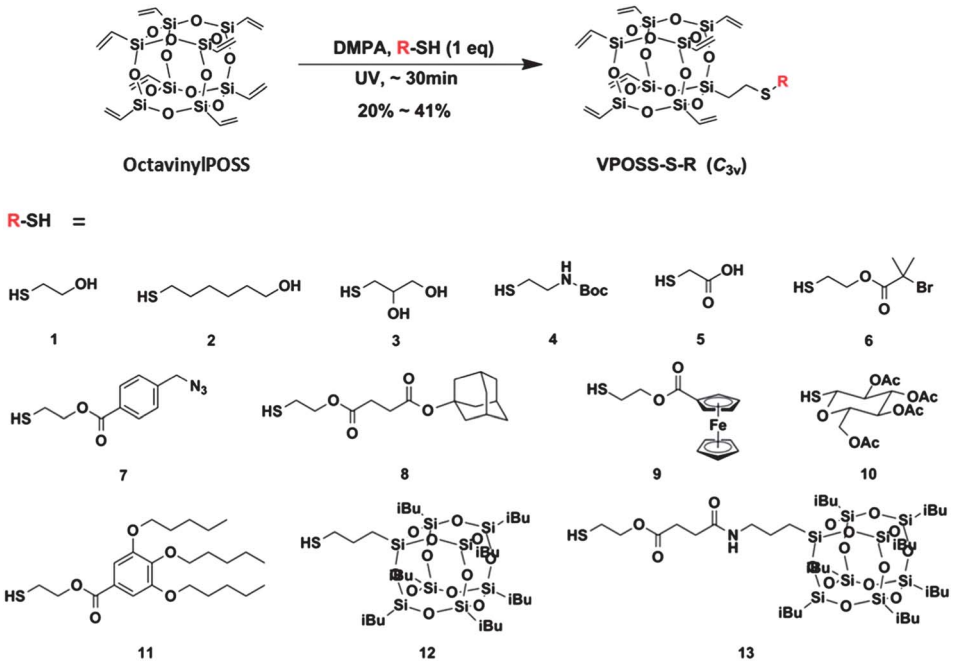

Scheme 1 General synthetic approach toward VPOSS-S-R **14–26** using thiol-ene chemistry (DMPA: 2,2-dimethoxy-2-phenylacetopheone).

structure. Fig. 1 summarizes the exemplary characterization of VPOSS-S-Br **19**. The product is a white powder readily soluble in common organic solvents such as $CHCl_3$ and THF. The introduction of a 2-bromoisobutyryl group and the formation of a thioether bond are evident from the appearance of a new peak at δ 1.94 ppm and a group of new peaks at δ 2.69–2.82 ppm in the ^{1}H NMR spectrum (Fig. 1a). The residual vinyl groups were confirmed by the resonances at δ 5.86–6.15 ppm in the ^{1}H NMR spectrum (Fig. 1a) and at δ 128.62 and 137.04 ppm in the ^{13}C NMR spectrum (Fig. 1b). In addition, the ^{29}Si NMR spectrum (Fig. 1c) clearly shows two resonances at δ −75.0 ppm (–$SiCHCH_2$) and −66.0 ppm (–$SiCH_2CH_2S$–), indicating a monofunctionalized product. Moreover, the peak observed at *m*/*z* 880.93 in the MALDI-TOF mass spectrum (Fig. 1d and Table 1) agrees well with the calculated monoisotopic molecular mass ($C_{22}H_{35}BrNaO_{14}SSi_8$, 880.90 Da). All the evidence confirms the successful synthesis of VPOSS-S-Br **19**. The characterization of the other VPOSS-S-R samples was performed similarly and the results can be found in the ESI.†

Table 1 summarises the experimental conditions, yields, and the molecular weights obtained from the MALDI-TOF mass spectra for each of the VPOSS-S-R derivatives reported in this work. Although some products showed more than one peak in the MALDI-TOF mass spectra (see ESI†), Table 1 only includes the *m*/*z* ratio and the corresponding calculated monoisotopic molecular mass for the peak corresponding to the sodium ion adduct of the whole molecule $(M{\cdot}Na)^+$. The full mass spectra have been provided in the ESI.† Regarding the reaction

Table 1 Summary of the VPOSS-S-R samples synthesized *via* thiol-ene reactions

Entry	Sample	Functional thiol	Reaction time	Yield	Molecular formula $(M{\cdot}Na)^+$	M (calcd; Da)	*m*/*z* (obsd)
1	VPOSS-S-OH (**14**)	2-Mercaptoethanol (**1**)	30 min	26%	$C_{18}H_{30}NaO_{13}SSi_8$	732.95	733.15
2	VPOSS-S-C_6-OH (**15**)	6-Mercapto-1-hexanol (**2**)	30 min	23%	$C_{22}H_{38}NaO_{13}SSi_8$	789.01	789.07
3	VPOSS-S-Di-OH (**16**)	1-Thioglycerol (**3**)	30 min	29%	$C_{19}H_{32}NaO_{14}SSi_8$	762.96	762.20
4	VPOSS-S-NH-Boc (**17**)	2-(Boc-amino)ethanethiol (**4**)	30 min	20%	$C_{23}H_{39}NNaO_{14}SSi_8$	832.01	832.11
5	VPOSS-S-COOH (**18**)	2-Mercaptoacetic acid (**5**)	30 min	25%	$C_{18}H_{28}NaO_{14}SSi_8$	746.94	746.96
6	VPOSS-S-Br (**19**)	Br-SH (**6**)	30 min	28%	$C_{22}H_{35}BrNaO_{14}SSi_8$	880.90	880.93
7	VPOSS-S-N_3 (**20**)	N_3-SH (**7**)	30 min	32%	$C_{26}H_{35}N_3NaO_{14}SSi_8$	891.99	892.05
8	VPOSS-S-AD (**21**)	AD-SH (**8**)	30 min	26%	$C_{33}H_{50}NaO_{16}SSi_8$	981.09	981.18
9	VPOSS-S-Fe (**22**)	Fe-SH (**9**)	60 min	20%	$C_{29}H_{38}FeNaO_{14}SSi_8$	944.94	945.06
10	VPOSS-S-Sugar (**23**)	Sugar-SH (**10**)	30 min	23%	$C_{30}H_{44}NaO_{21}SSi_8$	1019.01	1019.07
11	VPOSS-S-Dendron (**24**)	Dendron-SH (**11**)	30 min	36%	$C_{40}H_{64}NaO_{17}SSi_8$	1095.19	1095.31
12	VPOSS-S-BPOSS (**25**)	BPOSS-SH (**12**)	30 min	—[a]	$C_{47}H_{94}NaO_{24}SSi_{16}$	1545.21	1545.32
13	VPOSS-S-CONH-BPOSS (**26**)	BPOSS-NHCO-SH (**13**)	30 min	41%	$C_{53}H_{103}NNaO_{27}SSi_{16}$	1688.26	1688.30

[a] The monoadduct **25** could not be isolated due to the low polarity of the BPOSS-SH moiety.

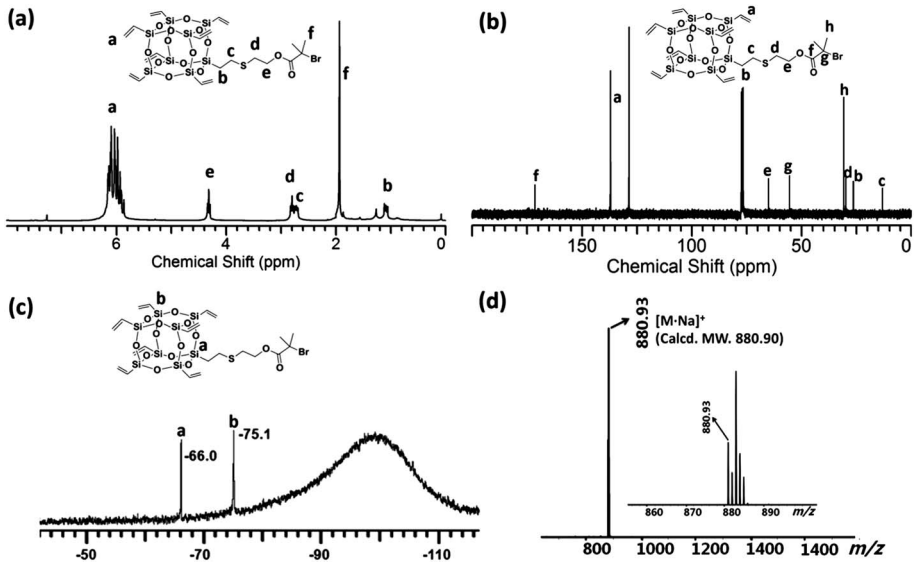

Fig. 1 Molecular characterization of VPOSS-S-Br **19** by its (a) ^{1}H NMR spectrum, (b) ^{13}C NMR spectrum, (c) ^{29}Si NMR spectrum, and (d) MALDI-TOF mass spectrum with a zoom-in view provided in the inset to show the corresponding isotope pattern.

conditions, it was observed that a slightly longer irradiation time (~1 hour, Table 1, entry 9) was required to prepare VPOSS-S-Fe. This may be explained by the fact that the ferrocene motif absorbs light of similar wavelength as DMPA, which reduces the initiation efficiency.[58] The yield of VPOSS-S-Fe was generally lower for this reason (~15% for 30 min irradiation and ~20% for 60 min irradiation).

One intriguing observation is that the yield of VPOSS-S-Dendron **24** (36%) is higher than those of the monoadduct products with smaller thiols (<30%). The quantities of tri-adducts and multi-adducts formed for VPOSS-S-Dendron **24** (<5%) are also lower than for the smaller thiols (usually >15%). The small thiols seem to be less selective, forming a statistical mixture of different addition products. This phenomenon suggests that steric effects influence the addition of thiol ligands to the octavinylPOSS cage. As a result, bulky functional thiols (such as Dendron-SH **11**) prefer to react with octavinylPOSS rather than with already formed adducts. Attached bulky ligands seem to present a significant steric hindrance by yielding more crowded POSS surfaces.

The reactions of BPOSS-SH **12** and BPOSS-NHCO-SH **13**, which are also bulky ligands, with octavinylPOSS appear to be selective as well. For BPOSS-SH **12**, it is difficult to isolate the unreacted octavinylPOSS, the monoadduct, the diadducts and the multi-adducts using flash chromatography due to the low polarity of BPOSS-SH **12**. Thus, we designed a thiol-functionalized POSS, BPOSS-NHCO-SH **13** with a longer spacer containing a polar amide bond. In this case, the monoadduct was successfully isolated in 41% yield, again confirming the role of steric hindrance in improving the selectivity for the mono-addition. The shape persistence and slightly larger size of the POSS motif seems to improve the selectivity when compared to Dendron-SH **11**. Notably, the diadducts were also isolated as a mixture of isomers in 22% yield. The MALDI-TOF mass spectrum confirms the diaddition (Fig. S11†), but we were unable to further separate the diadduct isomers with different symmetries by flash chromatography. We speculate that the steric effect of the thiol ligands are more profound for higher adducts. In other words, bulky ligands would tend to react with the vinyl groups at the *para*-position of the POSS cage where the steric hindrance is minimal. It is of great interest to investigate the functionalization selectivity in these higher adducts where the C_{3v} symmetry of mono-functional POSS building blocks is further changed.

Control over the size, symmetry, and function of POSS-based building blocks has received increasing research interest due to their wide-range applications from polymer chemistry to materials science. Using isomeric building blocks, it is possible to generate isomeric giant molecules with distinct supramolecular structures and unique physical properties. For example, it is interesting to investigate polymers constructed using solely *ortho*- or *para*-di-functional POSS building blocks as the repeating unit. The physical properties, such as the hydrodynamics volume, relaxation behavior and glass transition temperature are likely to be very different. However, regioselective multi-functionalization of POSS remains an immense challenge. Laine and co-workers have made pioneering work in this direction, as shown in the attempts to prepare Janus silsesquioxanes and mixed silsesquioxanes.[33,34] The mixture of regio-adducts is usually difficult to separate, especially in preparative quantities. We have found that electrospray ionization mass spectrometry (ESI) coupled with travelling wave ion mobility (TWIM) separation is particularly useful for the characterization of such mixtures with identical mass-to-charge ratio (m/z).[59–62] Previously, we have applied this method to determine the oligomeric states of a POSS–PDI–POSS conjugate where PDI stands for perylene diimide.[63] The method was found to be sensitive to the molecular conformation in the

three-dimensional space.[63] The principle of TWIM MS experiments is that ions of a given *m*/*z* travel through the TWIM cell under the influence of a pulsed electric field against the flow of a carrier gas (N_2). The ion drift times through the TWIM cell thus depend on the ions' charge and their collision cross-section (CCS) which are a reflection of the ion's size and shape (architecture). Hence, isomers with sufficiently different shapes can be separated even if they possess identical *m*/*z* values. Since mono-functional POSS does not have isomers and di-functional POSS has three isomers (*ortho*-, *meta*-, and *para*-), we challenged this method with the diadducts of thiol ligands and octavinylPOSS, namely VPOSS-(S-R)$_2$.

To prepare the diadducts, the reaction conditions were basically identical to those of the monoaddition reaction, except that two equivalents of thiols were used to maximize the diadduct products (*e.g.*, see Scheme 2). To reveal the exact composition of the diadducts, the crude product after the reaction was directly subjected to analysis by ESI coupled with TWIM separation. The diadducts are positional isomers with identical composition in terms of number and type of functional groups. Therefore, they should have the same ionization ability since the doubly-charged status is unlikely to affect their ionization ability as well.[71,72] Hence, there should be no enrichment and the analysis is thus not biased toward any specific components. The ESI-TWIM MS method also allows the quantification of the relative amounts of the different diadducts (*ortho*-, *meta*-, and *para*-isomers) if their cross-section areas and drift times are sufficiently different. It was found that the method failed to distinguish the diadduct isomers of different symmetries obtained from small thiol ligands. Interestingly, for bulky ligands, the diadducts from BPOSS-SH **12** can be clearly separated whereas the diadducts from BPOSS-NHCO-SH **13** could not be well resolved. This finding is reasonable since the diadduct isomers from BPOSS-NHCO-SH **13** have relatively long, flexible linkages between the POSS units. The differences among the CCS areas of these isomers are thus too small to be differentiated. Below, we focus on the diadducts from BPOSS-SH **12** (Scheme 2) and discuss the regio-selectivity during functionalization.

In the ESI-TWIM MS study, the doubly charged molecular ions at *m*/*z* 1247 were selected for ion mobility separation due to their high abundance. These ions have the composition of $[M\cdot 2O\cdot 2Na]^{2+}$ and originate from products in which the thioether groups have been oxidized to sulfoxide groups during the ionization process.[64] Three distinct species were successfully isolated from the ions of $[M\cdot 2O\cdot 2Na]^{2+}$ due to their different drift times, *viz.* 4.96, 5.87, and 6.59 ms (Fig. 2a). The isotope spacing ($\Delta m/z$) in their isotopic patterns is 0.5 amu, indicating that all isomers are in their doubly charged states (Fig. 2b). The CCS values deduced from the experimentally observed drift times (see ESI†) are 443, 468, and 486 Å^2 for the fractions drifting at 4.96, 5.87, and 6.59 ms, respectively (Table 2). Considering that more compact ions usually drift faster while more expanded ions always drift slower in ion mobility

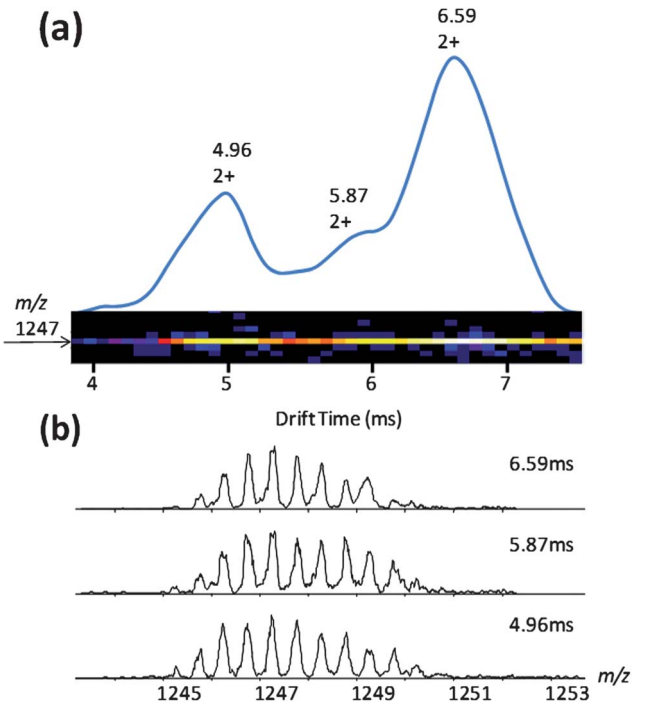

Fig. 2 Two-dimensional TWIM MS plots (relative intensity *vs.* drift time) of the ions at *m*/*z* 1247. (a) TWIM separation was performed using a traveling wave velocity of 350 m s^{-1}; the traveling wave height was 10 V. (b) The corresponding isotopic patterns for the three major peaks at 4.96, 5.87, and 6.59 ms. The ions are doubly charged species with the composition $[VPOSS\text{-}(S\text{-}BPOSS)_2\cdot 2O\cdot 2Na]^{2+}$.

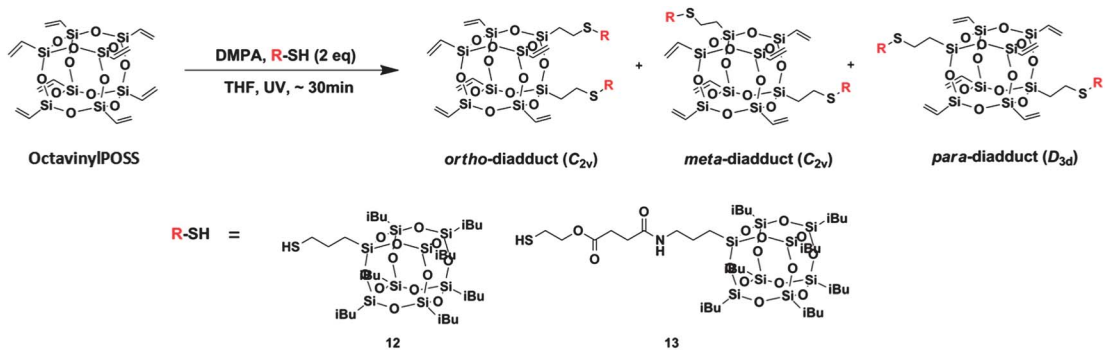

Scheme 2 Synthesis of the diadduct isomers VPOSS-(S-R)$_2$. DMPA stands for 2,2-dimethoxy-2-phenylacetopheone.

Table 2 Theoretical and experimental CCS values of the diadducts VPOSS-(S-BPOSS)$_2$

Isomer	Drift time (ms)	CCS_{calcd} (Å^2)	CCS_{exp} (Å^2)	Ratio
(*ortho*-)	4.96	453	443	21%
(*meta*-)	5.87	457	468	20%
(*para*-)	6.59	462	486	59%

experiments,[65–68] these three different species could probably be assigned to the *ortho*-, *meta*-, and *para*-isomers of the diadducts, respectively. The results from the molecular modeling with Materials Studio (version 4.2) were then employed to confirm the assignments.

Using the Anneal and Geometry Optimization tasks in the Forcite module, we generated 400 energy-minimized structures for each isomer through an annealing process to calculate the average CCS values by using the trajectory method of the MOBCAL algorithm, which is widely applied in calculations of large ion systems.[69] Plots of the resulting average CCS values against the corresponding relative energies are shown in Fig. S12† in order to identify all possible molecular conformations for each isomer. A representative structure of each isomer is given in Fig. 3. Na^+ was not included in the molecular simulations since cationizing metal ions usually have no significant effects on the average CCS values, especially for POSS-based giant molecules.[65,70] The average CCS values for each isomer were calculated to be 453 Å^2 for the *ortho*-diadduct, 457 Å^2 for the *meta*-diadduct, and 462 Å^2 for the *para*-diadduct (see Table 2). Both the order $CCS_{(ortho-)} < CCS_{(meta-)} < CCS_{(para-)}$ and the CCS values are qualitatively and quantitatively in good agreement with the experimental results, confirming that the isomers with drift times of 4.96 ms, 5.87 ms, and 6.59 ms result from the *ortho*-, *meta*- and *para*-isomers, respectively.

Based on the areas of the three distinct peaks observed after TWIM separation, we could estimate the relative composition of the three isomers in the mixture: *para*-compound (~59%), *meta*-compound (~20%), and *ortho*-compound (~21%). The majority of the diadducts has a *para* structure, while the *meta*- and *ortho*-compounds are minor products. This result suggests that there is significant steric hindrance when a large thiol ligand approaches the POSS tethered with one bulky substituent from the *ortho*- and *meta*-positions during the thiol-ene reaction. The *para*-position is the most favored site with minimal influence from the substituent. In contrast, such selectivity is not observed when small functional thiols are used. Therefore, thiol-ene chemistry is potentially a convenient way to achieve regio-selective multi-functionalization of octavinylPOSS. Although purification of the *ortho*-, *meta*-, and *para*-products at preparative scales has not been demonstrated in this study, it is anticipated that by using even bulkier thiols and engineering the properties of the ligands, the *para*-compounds may be sufficiently different from the *ortho*- and *meta*-isomers in terms of their physical properties, such as crystallinity and solubility, to warrant their separation in future studies.

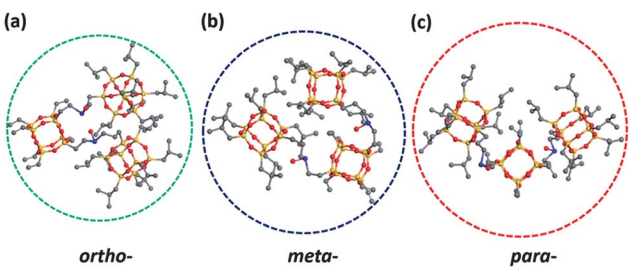

Fig. 3 Representative energy-minimized structures for the *ortho*-, *meta*-, and *para*-isomers of oxidized diadducts VPOSS-(S-BPOSS)$_2$ ([M·2O]) obtained by molecular modeling. The carbon atoms are grey, the silicon atoms are yellow, the oxygen atoms are red, and the sulfur atoms are blue.

Conclusions

In summary, we have successfully demonstrated a facile method to prepare POSS-based nanobuilding blocks with controlled symmetry breaking using thiol-ene chemistry. The stoichiometry-controlled reaction provides a straightforward and convenient access to a large variety of mono-functional POSS units. The selectivity for the monoaddition has been found to increase by using bulky thiol ligands. The synthesis of regio-selective multifunctional POSS derivatives has also been attempted. Analysis of the composition of the diadducts of VPOSS-(S-BPOSS)$_2$ by ESI-TWIM mass spectrometry revealed that the *para*-isomer constitutes 59% of the mixture, and the *ortho*- and *meta*-isomers are 21% and 20%, respectively. A study is ongoing in our laboratory to develop a library of mono-functional and multi-functional POSS nanobuilding blocks and to use them in the construction of various shape amphiphiles for the systematic study of their self-assembly principles and hierarchical structure formation in the bulk, thin films, and solutions.

Acknowledgements

This work was supported by the National Science Foundation (DMR-0906898 to S.Z.D.C. and CHE-1012636 to C.W.) and the Joint-Hope Education Foundation (to S.Z.D.C. and W.-B. Z.).

References

1 G. M. Whitesides and B. Grzybowski, *Science*, 2002, **295**, 2418.
2 J. D. Hartgerink, E. Beniash and S. I. Stupp, *Science*, 2001, **294**, 1684.
3 F. M. Menger and J. S. Keiper, *Angew. Chem., Int. Ed.*, 2000, **39**, 1906.
4 F. M. Menger and C. A. Littau, *J. Am. Chem. Soc.*, 1993, **115**, 10083.
5 L. Zhang and A. Eisenberg, *Science*, 1995, **268**, 1728.
6 F. S. Bates and G. H. Fredrickson, *Phys. Today*, 1999, **52**, 32.
7 S. Jiang, Q. Chen, M. Tripathy, E. Luijten, K. S. Schweizer and S. Granick, *Adv. Mater.*, 2010, **22**, 1060.

8 Y. Li, W.-B. Zhang, I.-F. Hsieh, G. Zhang, Y. Cao, X. Li, C. Wesdemiotis, B. Lotz, H. Xiong and S. Z. D. Cheng, *J. Am. Chem. Soc.*, 2011, **133**, 10712.
9 S. C. Glotzer and M. J. Solomon, *Nat. Mater.*, 2007, **6**, 557.
10 R. W. Date and D. W. Bruce, *J. Am. Chem. Soc.*, 2003, **125**, 9012.
11 S. C. Glotzer, M. A. Horsch, C. R. Iacovella, Z. Zhang, E. R. Chan and X. Zhang, *Curr. Opin. Colloid Interface Sci.*, 2005, **10**, 287.
12 W.-B. Zhang, Y. Li, X. Li, X. Dong, X. Yu, C.-L. Wang, C. Wesdemiotis, R. P. Quirk and S. Z. D. Cheng, *Macromolecules*, 2011, **44**, 2589.
13 X.-H. Dong, W.-B. Zhang, Y. Li, M. Huang, S. Zhang, R. P. Quirk and S. Z. D. Cheng, *Polym. Chem.*, 2012, **3**, 124.
14 W.-B. Zhang, Y. Tu, R. Ranjan, R. M. Van Horn, S. Leng, J. Wang, M. J. Polce, C. Wesdemiotis, R. P. Quirk, G. R. Newkome and S. Z. D. Cheng, *Macromolecules*, 2008, **41**, 515.
15 X. Yu, W.-B. Zhang, K. Yue, X. Li, H. Liu, Y. Xin, C.-L. Wang, C. Wesdemiotis and S. Z. D. Cheng, *J. Am. Chem. Soc.*, 2012, **134**, 7780.
16 Y. Han, Y. Xiao, Z. Zhang, B. Liu, P. Zheng, S. He and W. Wang, *Macromolecules*, 2009, **42**, 6543.
17 Y.-K. Han, Z.-J. Zhang, Y.-L. Wang, N. Xia, B. Liu, Y. Xiao, L.-X. Jin, P. Zheng and W. Wang, *Macromol. Chem. Phys.*, 2011, **212**, 81.
18 M. F. Roll, M. Z. Asuncion, J. Kampf and R. M. Laine, *ACS Nano*, 2008, **2**, 320.
19 K. Tanaka and Y. Chujo, *J. Mater. Chem.*, 2012, **22**, 1733.
20 S.-W. Kuo and F.-C. Chang, *Prog. Polym. Sci.*, 2011, **36**, 1649.
21 D. B. Cordes, P. D. Lickiss and F. Rataboul, *Chem. Rev.*, 2010, **110**, 2081.
22 G. Li, L. Wang, H. Ni and C. U. Pittman Jr, *J. Inorg. Organomet.Polym.*, 2001, **11**, 123.
23 X. Yu, K. Yue, I.-F. Hsieh, Y. Li, X.-H. Dong, C. Liu, Y. Xin, H.-F. Wang, A.-C. Shi, G. R. Newkome, R.-M. Ho, E.-Q. Chen, W.-B. Zhang and S. Z. D. Cheng, *Proc. Natl. Acad. Sci. U. S. A.*, 2013, **110**, 10078.
24 X. Yu, S. Zhong, X. Li, Y. Tu, S. Yang, R. M. Van Horn, C. Ni, D. J. Pochan, R. P. Quirk, C. Wesdemiotis, W.-B. Zhang and S. Z. D. Cheng, *J. Am. Chem. Soc.*, 2010, **132**, 16741.
25 K. Yue, C. Liu, K. Guo, X. Yu, M. Huang, Y. Li, C. Wesdemiotis, S. Z. D. Cheng and W.-B. Zhang, *Macromolecules*, 2012, **45**, 8126.
26 Z. Wang, Y. Li, X.-H. Dong, X. Yu, K. Guo, H. Su, K. Yue, C. Wesdemiotis, S. Z. D. Cheng and W.-B. Zhang, *Chem. Sci.*, 2013, **4**, 1345.
27 Y. Li, X.-H. Dong, K. Guo, Z. Wang, Z. Chen, C. Wesdemiotis, R. P. Quirk, W.-B. Zhang and S. Z. D. Cheng, *ACS Macro Lett.*, 2012, **1**, 834.
28 H. Su, J. Zheng, Z. Wang, F. Lin, X. Feng, X.-H. Dong, M. L. Becker, S. Z. D. Cheng, W.-B. Zhang and Y. Li, *ACS Macro Lett.*, 2013, **2**, 645.
29 Y. Li, Z. Wang, J. Zheng, H. Su, F. Lin, K. Guo, X. Feng, C. Wesdemiotis, M. L. Becker, S. Z. D. Cheng and W.-B. Zhang, *ACS Macro Lett.*, 2013, **2**, 1026.
30 A. Hirsch and M. Brettreich, *Fullerenes: Chemistry and Reactions*, Wiley-VCH, Weinheim, Great Britain, 2005.
31 Y. Matsuo and E. Nakamura, *Chem. Rev.*, 2008, **108**, 3016.
32 F. Giacalone and N. Martin, *Chem. Rev.*, 2006, **106**, 5136.
33 M. Z. Asuncion and R. M. Laine, *J. Am. Chem. Soc.*, 2010, **132**, 3723.
34 M. Z. Asuncion, M. Ronchi, H. Abu-Seir and R. M. Laine, *C. R. Chim.*, 2010, **13**, 270.
35 E. G. Shockey, A. G. Bolf, P. F. Jones, J. J. Schwab, K. P. Chaffee, T. S. Haddad and J. D. Lichtenhan, *Appl. Organomet. Chem.*, 1999, **13**, 311.
36 C. Marcolli and G. Calzaferri, *Appl. Organomet. Chem.*, 1999, **13**, 213.
37 A. Tsuchida, C. Bolln, F. G. Sernetz, H. Frey and R. Mülhaupt, *Macromolecules*, 1997, **30**, 2818.
38 P. A. Agaskar, *Inorg. Chem.*, 1991, **30**, 2707.
39 F. J. Feher, D. A. Newman and J. F. Walzer, *J. Am. Chem. Soc.*, 1989, **111**, 1741.
40 F. J. Feher, *J. Am. Chem. Soc.*, 1986, **108**, 3850.
41 F. J. Feher, K. D. Wyndham, R. K. Baldwin, D. Soulivong, J. D. Lichtenhan and J. W. Ziller, *Chem. Commun.*, 1999, 1289.
42 P.-O. M. Eugenia, B. Trastoy, A. Rol, M. D. Chiara, I. Garcia-Moreno and J. L. Chiara, *Chem.–Eur. J.*, 2013, **19**, 6630.
43 B. Trastoy, P.-O. M. Eugenia, R. Sastre and J. L. Chiara, *Chem.–Eur. J.*, 2010, **16**, 3833.
44 J. Xu, X. Li, C. M. Cho, C. L. Toh, L. Shen, K. Y. Mya, X. Lu and C. He, *J. Mater. Chem.*, 2009, **19**, 4740.
45 Y. Gao, A. Eguchi, K. Kakehi and Y. C. Lee, *Org. Lett.*, 2004, **6**, 3457.
46 C. E. Hoyle and C. N. Bowman, *Angew. Chem., Int. Ed.*, 2010, **49**, 1540.
47 A. B. Lowe, *Polym. Chem.*, 2010, **1**, 17.
48 M. J. Kade, D. J. Burke and C. J. Hawker, *J. Polym. Sci., Part A: Polym. Chem.*, 2010, **48**, 743.
49 Y. Li, W.-B. Zhang, J. E. Janoski, X. Li, X. Dong, C. Wesdemiotis, R. P. Quirk and S. Z. D. Cheng, *Macromolecules*, 2011, **44**, 3328.
50 A. K. Tucker-Schwartz, R. A. Farrell and R. L. Garrell, *J. Am. Chem. Soc.*, 2011, **133**, 11026.
51 V. Ervithayasuporn, X. Wang and Y. Kawakami, *Chem. Commun.*, 2009, 5130.
52 L.-Q. Gu, S. Cheley and H. Bayley, *Science*, 2001, **291**, 636.
53 J. Li and X. J. Loh, *Adv. Drug Delivery Rev.*, 2008, **60**, 1000.
54 C. Wang, Z. Wang and X. Zhang, *Acc. Chem. Res.*, 2012, **45**, 608.
55 D. R. van Staveren and N. Metzler-Nolte, *Chem. Rev.*, 2004, **104**, 5931.
56 A. Harada, *Acc. Chem. Res.*, 2001, **34**, 456.
57 B. M. Rosen, C. J. Wilson, D. A. Wilson, M. Peterca, M. R. Imam and V. Percec, *Chem. Rev.*, 2009, **109**, 6275.
58 A. Thander and B. Mallik, *Chem. Phys. Lett.*, 2000, **330**, 521.
59 E. S. Baker, J. Gidden, S. E. Anderson, T. S. Haddad and M. T. Bowers, *Nano Lett.*, 2004, **4**, 779.
60 E. Van Duijn, A. Barendregt, S. Synowsky, C. Versluis and A. J. R. Heck, *J. Am. Chem. Soc.*, 2009, **131**, 1452.
61 S. D. Pringle, K. Giles, J. L. Wildgoose, J. P. Williams, S. E. Slade, K. Thalassinos, R. H. Bateman, M. T. Bowers and J. H. Scrivens, *Int. J. Mass Spectrom.*, 2007, **261**, 1.

62 Y.-T. Chan, X. Li, J. Yu, G. A. Carri, C. N. Moorefield, G. R. Newkome and C. Wesdemiotis, *J. Am. Chem. Soc.*, 2011, **133**, 11967.
63 X. Ren, B. Sun, C.-C. Tsai, Y. Tu, S. Leng, K. Li, Z. Kang, R. M. V. Horn, X. Li, M. Zhu, C. Wesdemiotis, W.-B. Zhang and S. Z. D. Cheng, *J. Phys. Chem. B*, 2010, **114**, 4802.
64 J. W. Chan, B. Yu, C. E. Hoyle and A. B. Lowe, *Polymer*, 2009, **50**, 3158.
65 S. E. Anderson, C. Mitchell, T. S. Haddad, A. Vij, J. J. Schwab and M. T. Bowers, *Chem. Mater.*, 2006, **18**, 1490.
66 L. A. Angel, L. T. Majors, A. C. Dharmaratne and A. Dass, *ACS Nano*, 2010, **4**, 4691.
67 D. P. Smith, S. E. Radford and A. E. Ashcroft, *Proc. Natl. Acad. Sci. U. S. A.*, 2010, **107**, 6794.
68 B. T. Ruotolo, J. L. P. Benesch, A. M. Sandercock, S.-J. Hyung and C. V. Robinson, *Nat. Protoc.*, 2008, **3**, 1139.
69 A. A. Shvartsburg and M. F. Jarrold, *Chem. Phys. Lett.*, 1996, **261**, 86.
70 S. E. Anderson, E. S. Baker, C. Mitchell, T. S. Haddad and M. T. Bowers, *Chem. Mater.*, 2005, **17**, 2537.
71 P. Wang, G. Wesdemiotis, C. Kapota and G. Ohanessian, *J. Am. Soc. Mass Spectrom.*, 2007, **18**, 541.
72 M. Rozman and S. J. Gaskell, *J. Mass Spectrom.*, 2010, **45**, 1409.